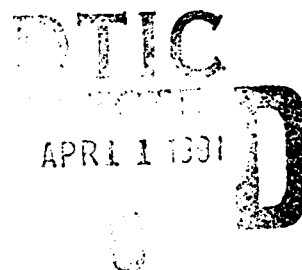**aval Research Laboratory**

shington, DC 20375-5000

AD-A233 387

Theory of Electron Beam Tracking
In Reduced-Density Channels

R. F. FERNSLER, S. P. SLINKER AND R. F. HUBBARD

Beam Physics Branch
Plasma Physics Division

April 2, 1991

REPORT DOCUMENTATION PAGE

Form Approved
OMB No. 0704-0188

1. AGENCY USE ONLY *(Leave blank)*	2. REPORT DATE	3. REPORT TYPE AND DATES COVERED
	1991 April 2	Interim

4. TITLE AND SUBTITLE

Theory of Electron Beam Tracking in Reduced-Density Channels

5. FUNDING NUMBERS

JO#47-0900-0-1

6. AUTHOR(S)

R. F. Fernsler, S. P. Slinker, and R. F. Hubbard

7. PERFORMING ORGANIZATION NAME(S) AND ADDRESS(ES)

Naval Research Laboratory
Washington, DC   20375-5000

8. PERFORMING ORGANIZATION REPORT NUMBER

NRL Memorandum
Report 6806

9. SPONSORING/MONITORING AGENCY NAME(S) AND ADDRESS(ES)

DARPA   NSWC
Arlington, VA   22209   Silver Spring, MD   20903-5000

10. SPONSORING/MONITORING AGENCY REPORT NUMBER

11. SUPPLEMENTARY NOTES

12a. DISTRIBUTION/AVAILABILITY STATEMENT

Approved for public release; distribution unlimited.

12b. DISTRIBUTION CODE

13. ABSTRACT *(Maximum 200 words)*

A theory is presented for the guiding of relativistic electron beams by rarefied gaseous channels. The analysis is based on analytic computations of the transverse force felt by a rigid-rod beam propagating off-axis from a channel or reduced gas density. The density gradients produce an attractive channel force that can be surprisingly robust, even though it develops from relatively subtle gas chemistry properties. Static numerical calculations support the analytic work. Longitudinal beam coupling and effects that degrade channel guidance are discussed as well.

14. SUBJECT TERMS

Relativistic electron beam   Hose instability
Tracking   Reduced Gas Density
Longitudinal coupling

15. NUMBER OF PAGES

52

16. PRICE CODE

17. SECURITY CLASSIFICATION OF REPORT	18. SECURITY CLASSIFICATION OF THIS PAGE	19. SECURITY CLASSIFICATION OF ABSTRACT	20. LIMITATION OF ABSTRACT
Unclassified	Unclassified	Unclassified	SAR

CONTENTS

THEORY OF ELECTRON BEAM TRACKING
IN REDUCED-DENSITY CHANNELS

I. INTRODUCTION

The propagation of a charged particle beam through a dense gas is
degraded by collisions with the gas molecules.[1] This degradation limits
the useful range of charged particle beams, and thus limits their utility
in applications such as electron-beam welding,[2,3] directed-energy weapons,[4]
and inertial confinement fusion reactors.[5,6] One means of extending the
range in a given environment is to create a reduced-density channel using
previous beam pulses or external means to heat the gas. The heated gas
expands to reach pressure balance with the background gas, leaving a
long-lived rarefied channel that can dramatically enhance the range of
subsequent beam pulses.

To benefit from the channel, the beam must remain inside. Thus, the
deflection forces produced by the channel on the beam are important. This
importance has been demonstrated in experiments using beams injected into
hot, highly ionized channels. These channels quickly expel the beam
through beam-induced return currents.[7] Rarefied but highly conducting
channels do not, therefore, benefit the beam, unless strong external guide
fields are provided.

An attractive force that keeps the beam in the channel would be ideal.
An electrostatic force produced by low-level channel preionization has been
proposed by Lee,[8] but this force is weak, short-lived, partially repulsive,
and has never been observed experimentally.[9,10] Much more important is the

magnetic channel force recently discovered by Welch[11] in simulations of electron beams propagating through initially un-ionized air. The attraction between the low-density channel and the beam results from beam impact ionization and an electrical conductivity dependent on the plasma electron temperature. The higher temperature in the rarefied channel depresses the conductivity and return current in the channel, thus shifting the centroid of the net current toward the channel axis. Magnetic attraction between the beam current and net current pulls the beam into the channel. This attraction has been observed experimentally by Murphy et al.[12] using deep, discharge-produced channels, and by Bieniosek using a double-pulse electron beam, as reported in Ref. 11.

In this paper we provide a theoretical basis for electron beam guiding by density channels. In particular, we derive analytic formulas for the net deflection force produced by an initially un-ionized, reduced-density channel on a rigid-rod, azimuthally symmetric, ultrarelativistic electron beam. We assume for simplicity that the channel gas density is sufficiently high that a scalar conductivity adequately describes its electrical properties. Our analysis shows that the density-channel force is strong and long-lived, and that it interlaces well with the longitudinal coupling force binding the beam body to the head. The density-channel force thus appears capable of keeping a (stable) beam in a channel, without ancillary fields or forces. Effects that degrade tracking, including higher-order chemistry and channel preionization, are discussed as well. Numerical simulations using a nonlinear particle code confirm the analytic results. In future work, we will present dynamical simulations that describe the actual response of the beam to the channel.

II. GENERAL DESCRIPTION: THEORY AND EXPERIMENT

A. Physical Mechanism

External currents or charges can deflect a beam provided they are distributed asymmetrically about the beam. For a beam passing through a neutral gas, the electrical conductivity of the gas must be azimuthally asymmetric with respect to the beam, either through gradients in the gas ionization or gradients in the gas density. In this study, we consider beam deflection arising from the density gradients of a rarefied channel. For simplicity, we assume that the heavy gas molecules and ions are immobile during each short beam pulse. We additionally assume that the dominant source of ionization is beam impact ionization (including that from the energetic secondaries), and that it is a local and instantaneous process. Other mechanisms of ionization and deionization are considered separately in Sec. V-B.

To understand how a density channel can deflect a beam, let us write the conductivity of a weakly ionized gas as

$$\sigma = \frac{e^2 n}{mN\nu_m} ,$$
(1)

where n is the number density of the plasma electrons, $N\nu_m$ is their momentum-transfer collision frequency, m and e are the electron mass and charge, respectively, and N is the gas number density. The reduced collision frequency, ν_m, equals an average of the plasma-electron speed times the cross section for momentum transfer to the gas molecules. In a weakly ionized gas, ν_m is a function only of the plasma electron temperature T_e, and it rises with T_e for most gases.

Conductivity is generated as the beam electrons collide with and ionize the gas molecules. The collision rate is proportional to the gas density

N, and hence the degree of ionization, n/N, is independent of N and is symmetric about the beam. Asymmetry in σ can then arise only through ν_m and its dependence on T_e. Asymmetry in T_e and a temperature-dependent collision frequency are thus needed to produce beam deflection.

The temperature T_e is determined by the heating and cooling rates of the plasma electrons. The temperature is high in low-density regions where the collisional cooling rate (proportional to N) is reduced. In most gases, the elevated temperature raises ν_m and lowers σ. This preferential reduction in plasma conductivity lowers the plasma return current flowing in the channel. The density depression thus produces a perturbed channel current that flows parallel to the beam current and attracts it magnetically. The channel force is attractive and long-lived as long as n/N is symmetric about the beam and ν_m rises with T_e. A mathematical formulation of this model is given in Sec. III-A. First, however, we briefly review the existing experimental evidence for the effect.

B. Tracking Experiments

Experiments at the Naval Research Laboratory by Murphy et al.[12] and at McDonnell-Douglas Research Laboratory by Bieniosek[11] have confirmed that electron beams are attracted to density channels. Murphy et al. propagated a 1 MeV, 10 kA, 35 ns electron beam from the Pulserad 310 generator into a channel formed by an electrical discharge. The discharge was directed through roughly two meters of air at 760 torr using a Nd::glass laser to prepare a weakly preionized path. The discharge could be displaced up to three cm from the beam axis, and it produced a channel that grew to several cm in radius at pressure equilibrium. The effect of the channel on the electron beam was ejection from hot channels and attraction toward cool

4

channels. This behavior is expected because hot channels are highly conducting while cool channels are not. Although the tracking effect was unambiguous, precise quantitative measurements were hampered by large hose growth and uncertainties in the channel parameters. Continuing experiments are being performed using the 5 MeV SuperIBEX generator.[13]

The experiments of Bieniosek[11] were performed on the two-pulse MEDEA II device. The parameters of each pulse were similar to those of Pulserad, and a variety of pulse separation times, gas mixtures and gas densities were employed. The first pulse was deflected by a transverse magnetic field that was turned off prior to injection of the second pulse. Attraction of the second pulse to the density channel formed by the first pulse demonstrated the effect. Since the density reduction was modest, the attraction was much weaker than in the Pulserad experiments.

III. TRACKING FORMALISM

A. Force Equation

In this section we derive formulas for the magnetic deflection force produced by an initially un-ionized density channel on an ultrarelativistic electron beam. The force is termed tracking if it pulls the beam toward the channel, and detracking if it pushes the beam away. To simplify the analysis, we assume that the beam is azimuthally symmetric about a common axis, and we ignore axial and temporal variations relative to transverse variations to order $\partial/\partial z$, $\partial/\partial\zeta \ll 1/r_b$; here r_b is a characteristic beam radius, and $\zeta = ct-z$ measures distance behind the beam head. The force equation then reduces to a static, two-dimensional calculation, with the beam and plasma treated as infinitely long at each location ζ. To this order of approximation, there is no transverse current flow. Furthermore,

5

because an infinitely long, azimuthally symmetric ring of beam current produces no fields or forces inside itself, the ring can feel, by reciprocity, no net force from currents and charges inside. Hence, only currents and charges outside the ring can deflect it. See Fig. 1.

Consider now a plasma return current of density σE_z, where E_z is the axial electric field. In the direction linking the beam and channel axes, $\theta = 0$, this current magnetically deflects a beam ring of radius r and current δI_b with a distributed net force given by the Biot-Savart law:

$$F_m(r,\zeta) \, dr \;=\; \delta I_b(r,\zeta) \int_r^{\infty} dr' \; r' \int_0^{2\pi} d\theta \; \cos\theta \; \frac{2\sigma E_z}{r'c^2} \;, \qquad (2)$$

where $\delta I_b(r,\zeta) = 2\pi r \, dr \, j_b(r,\zeta)$ and j_b is the beam current density. Summing over all beam rings and integrating by parts yields the average force per beam electron:

$$F_{tm}(\zeta) \;=\; \frac{ec}{I_b} \int_0^{\infty} dr \; F_m(r,\zeta)$$

$$=\; \frac{2e}{c} \int_0^{\infty} dr \; \frac{\partial i_b}{\partial r} \int_r^{\infty} dr' \int_0^{2\pi} d\theta \; \cos\theta \; \sigma E_z$$

$$=\; \frac{2e^3}{mc} \int_0^{\infty} dr \; i_b \left(\frac{n}{N}\right) \int_0^{2\pi} d\theta \; \cos\theta \; \frac{E_z}{\nu_m} \;, \qquad (3)$$

where I_b is the total beam current and

$$i_b(r,\zeta) \;=\; \int_0^{r} dr \; 2\pi r \; \frac{j_b(r,\zeta)}{I_b(\zeta)} \qquad (4)$$

6

is the fraction of beam current within radius r. In deriving Eq. (3), we have invoked definition (1) for σ and assumed that n/N is symmetric about the beam.

As shown in Sec. IV-A, the field E_z soon becomes azimuthally symmetric, and hence it can be pulled outside the integral over θ. We can then rewrite the angular integral by invoking the assumption that ν_m depends on θ only through its dependence on N:

$$\int_0^{2\pi} d\theta \, \frac{\cos\theta}{\nu_m} = -\int_0^{2\pi} d\theta \, \sin\theta \, \frac{\partial}{\partial\theta} \left(\frac{1}{\nu_m}\right)$$

$$= \int_0^{2\pi} d\theta \, \sin\theta \, \frac{q}{\nu_{mo}} \, \frac{\partial}{\partial\theta} \ln(N_o/N), \tag{5}$$

where N_o is the ambient gas density outside the channel, and we define

$$q = -\frac{\partial(\nu_{mo}/\nu_m)}{\partial\ln(N_o/N)} . \tag{6}$$

Here ν_{mo} is a characteristic value of the reduced collision frequency. If we now assume, as discussed in Sec. V-A, that q is a gas parameter independent of (r,θ), we can rewrite force equation (3) as

$$F_{tm}(\zeta) = \frac{2eq}{c} \int_0^\infty dr \, i_b \, \sigma_o E_z \int_0^{2\pi} d\theta \, \sin\theta \, \frac{\partial}{\partial\theta} \ln(N_o/N) , \tag{7}$$

where $\sigma_o(r,\zeta) = e^2 n/mN\nu_{mo}$.

B. Linearized Analysis

Consider first a small channel offset, y_c, satisfying

$$y_c \ll r_b, \ r_c, \tag{8}$$

where r_b is the beam radius and r_c is the channel radius. We can then expand the gas density about the beam axis as

$$\ln\left[N_o/N(r,\theta)\right] = \ln\left[N_o/N(r)\right] - y_c\cos\theta \frac{\partial}{\partial r} \ln\left[N_o/N(r)\right] + \ldots \tag{9}$$

This approximation reduces force equation (7) to

$$F_{tm}(\zeta) = \frac{2\pi e}{c} qy_c \int_0^\infty dr \ i_b \ \sigma_o E_z \frac{\partial}{\partial r} \ln(N_o/N) \ , \tag{10}$$

with the solution determined by the radial distributions of the beam current, the plasma current, and the density channel.

A particularly simple example is a square density channel for which $N = N_c$ for $r < r_c$ and $N = N_o$ for $r > r_c$. Then,

$$F_{tm}(\zeta) = \frac{2\pi e}{c} qy_c \ln(N_o/N_c) \ f(r_c,\zeta) \ j_b(r_c,\zeta) \ i_b(r_c,\zeta) \ , \tag{11a}$$

where the plasma return-current fraction, $f = -\sigma_o E_z/j_b$, is positive for rising or constant $I_b(\zeta)$. If the beam and its ionization take self-similar Bennett profiles of the form $j_b(r,\zeta) = I_b(\zeta)r_b^2/\pi(r^2+r_b^2)^2$ and $i_b(r,\zeta) = r^2/(r^2+r_b^2)$, Eq. (11a) reduces to

$$F_{tm}(\zeta) = qf \frac{2eI_b}{r_b c} \frac{y_c}{r_b} \ln(N_o/N_c) \frac{r_c^2/r_b^2}{(1 + r_c^2/r_b^2)^3} \ . \tag{11b}$$

Several features can be deduced from these results. First, the tracking force can be large and even exceed the magnetic self-pinch force, $F_o = e(1-f)I_b/r_b c$, that holds the beam together. Although the beam is

8

likely to distort azimuthally when $F_{tm} \gtrsim F_o$, such distortion should not disrupt channel tracking. Moreover, $F_{tm} \ll F_o$ in most applications, and the rigid-rod treatment is then well justified. Second, the sign of F_{tm} is independent of the relative sizes of the beam and channel, and it is tracking, $F_{tm}/y_c > 0$, provided $q,f > 0$ and $N_o > N_c$. Third, F_{tm} has a broad maximum when the beam and channel radii are comparable, but diminishes rapidly as the channel becomes much smaller or larger than the beam. Fourth, F_{tm} is long-lived, persisting as long as plasma return current flows at the channel edge. And fifth, F_{tm} depends logarithmically on the channel gas density. This weak dependence suggests that deep channels are not needed to effect strong tracking. Only in shallow channels, $(N_o - N_c) \ll N_o$, is the force is sensitive to the channel depth, $F_{tm} \propto (N_o - N_c)$.

For small offsets, the tracking force varies linearly with y_c. This suggests that the characteristic axial distance needed to pull the beam into the channel is given by the harmonic-oscillator result:

$$z_t = \frac{\pi}{2} \left[\frac{\gamma mc^2}{F_{tm}/y_c} \right]^{1/2} , \tag{12}$$

where γ is the relativistic mass factor for the beam. Using force equation (11b),

$$z_t = \frac{\lambda_{\beta o}}{4} \left[\left(\frac{1-f}{f} \right) \left(\frac{r_b}{r_c} \right)^2 \frac{(1 + r_c^2/r_b^2)^3}{2q \, \ln(N_o/N_c)} \right]^{1/2} , \tag{13}$$

where $\lambda_{\beta o} = 2\pi r_b [I_A/(1-f)I_b]^{1/2}$ is an average betatron oscillation wavelength[1] for the beam electrons, and $I_A = \gamma mc^3/e \simeq 17\gamma$ kA is the beam Alfven current.

9

C. Nonlinear Analysis

A linear analysis simplifies the mathematics but is restricted to small offsets y_c. For completeness, we present a nonlinear analysis valid for arbitrary offset. We also choose a more realistic, rounded profile for the channel gas density that is amenable to numerical treatment:

$$N(r') = N_0 \left[\frac{(r'/r_c)^2 + \delta}{(r'/r_c)^2 + 1} \right]^p, \tag{14}$$

where $r'^2 = r^2 + y_c^2 - 2ry_c\cos\theta$, and $\delta < 1$ and $p > 0$ are constants. In the channel center, $N(0) = N_c = N_0 \delta^p$.

Profile (14) is easily differentiated in force equation (7):

$$\frac{\partial}{\partial\theta} \ln(N_0/N) = p \frac{\partial}{\partial\theta} \ln\left[\frac{r^2 + y_c^2 - 2y_c r \cos\theta + r_c^2}{r^2 + y_c^2 - 2y_c r \cos\theta + r_c^2 \delta} \right]$$

$$= \frac{2py_c r \sin\theta}{r^2 + y_c^2 - 2y_c r \cos\theta + r_c^2} - \frac{2py_c r \sin\theta}{r^2 + y_c^2 - 2y_c r \cos\theta + r_c^2 \delta}. \tag{15}$$

The integral over θ can then be performed using the general result that

$$\int_0^{2\pi} d\theta \, \frac{\sin^2\theta}{a - b\cos\theta} = 2\pi \frac{a - \sqrt{a^2 - b^2}}{b^2}, \tag{16}$$

for $a \geq b$. After considerable algebra, this reduces Eq. (7) to

$$F_{tm}(\zeta) = -\frac{2\pi eqp}{y_c c} \int_0^\infty \frac{dr}{r} \, i_b \, \sigma_o E_z \left\{ (1 - \delta)r_c^2 \right.$$

$$+ \left[r^4 + 2r^2(r_c^2\delta - y_c^2) + (y_c^2 + r_c^2\delta)^2 \right]^{1/2}$$

$$\left. - \left[r^4 + 2r^2(r_c^2 - y_c^2) + (y_c^2 + r_c^2)^2 \right]^{1/2} \right\}. \tag{17}$$

10

Consider now a beam with a Bennett profile of constant radius r_b. The degree of ionization, n/N, produced by impact ionization is then self-similar with the beam. We also assume that E_z is independent of radius r, which is usually a fair approximation as discussed in Sec. IV-A. The assumption that q and ν_{mo} are independent of (r,θ) implies that the reduced collision frequency takes the peculiar form

$$\nu_m(r,\theta,\zeta) = \frac{\nu_{mo}(\zeta)}{1 - \ln\left([N_o/N(r,\theta)]^q\right)} . \tag{18}$$

This form is valid only if q < 1 and the minimum gas density exceeds $N_o \exp(-1/q)$. The validity of Eq. (18) and typical values for q and ν_{mo} are discussed in Sec. V-A.

With these assumptions, Eq. (17) can be integrated. The result is

$$F_{tm}(\zeta) = \frac{qp}{2k} \frac{eI_p}{y_c c} \left[g(1) - g(\delta)\right] , \tag{19}$$

where I_p is the total plasma return current and k and g are defined through the relationships

$$g(\delta) = \frac{(2r_b r_c y_c)^2}{d(\delta)^6} \delta \ln[\alpha(\delta)] + \frac{y_c^4 - (r_b^2 - r_c^2\delta)^2}{d(\delta)^4} , \tag{20a}$$

$$d(\delta) = \left[(y_c^2 + r_c^2\delta)^2 + 2r_c^2(y_c^2 - r_c^2\delta) + r_b^4\right]^{1/4} , \tag{20b}$$

$$\alpha(\delta) = \frac{[d(\delta)^2 + r_c^2\delta - y_c^2 - r_b^2)r_b^2}{(y_c^2 + r_c^2\delta)d(\delta)^2 + (y_c^2 + r_c^2\delta)^2 + (y_c^2 - r_c^2\delta)r_b^2} , \tag{20c}$$

$$k(\delta) = 1 + \frac{pq}{2} \left[\ln(\delta) + g_1(1) - g_1(\delta)\right] , \tag{20d}$$

and

$$g_1(\delta) \;=\; \frac{y_c^{\,2} + r_c^{\,2}\delta + r_b^{\,2}}{d(\delta)^2}\,\ln[\alpha(\delta)].\tag{20e}$$

Equation (20d) for the normalization coefficient k was obtained using the definition of the plasma return current,

$$I_p \;=\; \int\limits_0^{\infty} dr\; r\; \frac{e^2}{m}\left(\frac{n}{N}\right) E_z \int\limits_0^{2\pi} d\theta\, \frac{1}{\nu_m}\,,\tag{21}$$

where n/N has the same Bennett profile as the beam, and E_z is again assumed to be independent of r.

The nonlinear result (19)-(20) offers generality at the expense of complexity. The principal additional information is that F_{tm} peaks when the beam lies at the channel edge (where $\partial\ln[N_o/N]/\partial r'$ peaks), and that F_{tm} remains tracking and falls off nearly quadratically with y_c when $y_c \gg r_c$. (The fall-off is faster, however, if the beam or channel is sharp-edged; for example, F_{tm} equals zero if the beam is entirely outside the channel.) The nonlinear result also confirms that F_{tm} rises nearly linearly with the chemistry parameter q and weakly with the channel depth. These dependencies are shown in Fig. 2.

IV. FIELD EQUATIONS

A. Neglecting the Dipole Electric Field

The preceding tracking analysis is predicated on the assumption that the electric field is symmetric about the beam and varies weakly with radius r. Here we justify that assumption in the high-conductivity region where the plasma return current and magnetic tracking are important. In

12

this region, the electrostatic potential and transverse electric field are shorted out, leaving an axial electric field given by

$$E_z = -\frac{\partial A}{\partial \zeta} .$$ (22)

The axial vector potential A and field E_z are determined by the Lorentz wave equation, given in the frozen-field limit by[14]

$$\nabla_\perp^2 A = -\frac{4\pi}{c} \left[j_b + \sigma E_z \right] .$$ (23)

The behavior of E_z is most easily analyzed using the linearization employed in Sec. III-B. For small channel offsets, the vector potential can be expanded in terms of monopole and dipole components:

$$A(r,\theta,\zeta) = A_o(r,\zeta) + A_1(r,\zeta) \cos\theta + \ldots$$ (24)

We again consider ohmic heating only, but for convenience, we replace Eq. (18) with the modified form,

$$\nu_m(r,\theta,\zeta) = \nu_{mo} \left[\frac{E_z(r,\theta,\zeta)}{N(r,\theta)} \frac{N_o}{E_o} \right]^{\bar{q}} ,$$ (25)

where $\bar{q}$ is constant and E_o/N_o is a reference field strength. Imposing expansion (9) for N and expansion (24) for A on Eqs. (22), (23) and (25) produces, after some manipulation, the linearized equations

$$\left[\frac{1}{r} \frac{\partial}{\partial r} r \frac{\partial}{\partial r} - \frac{4\pi}{c} \bar{\sigma} \frac{\partial}{\partial \zeta} \right] A_o = -\frac{4\pi}{c} j_b(r,\zeta) ,$$ (26)

and

$$\left[\frac{\partial}{\partial r} \frac{1}{r} \frac{\partial}{\partial r} r - \frac{4\pi}{c} (1-\bar{q}) \bar{\sigma} \frac{\partial}{\partial \zeta} \right] A_1 = \frac{4\pi}{c} \bar{q} \, y_c \, \bar{\sigma} \frac{\partial A_o}{\partial \zeta} \frac{\partial}{\partial r} \ln(N_o/N) ,$$ (27)

13

where the monopole conductivity $\bar{\sigma}(r,\zeta)$ is computed using $E_z = -\partial A_0/\partial\zeta$ in Eq. (25) for ν_m.

The characteristic relaxation length for the monopole potential A_0 can be determined from Eq. (26). For self-similar Bennett profiles, this length is given by

$$\zeta_{mo} = \frac{\pi\bar{\sigma}(0,\zeta)r_b^2}{c} \ln\left(1 + b^2/r_b^2\right) , \qquad (28)$$

where $\bar{\sigma}(0,\zeta)$ is the on-axis monopole conductivity, and $b \gg r_b$ is the radius within which space-charge neutralization occurs. The monopole potential in this case is given by

$$A_0(r,\zeta) = \frac{(1-f)I_b}{c} \ln\left(\frac{b^2 + r_b^2}{r^2 + r_b^2}\right) , \qquad (29)$$

where f is the plasma return-current fraction. The weak, logarithmic dependence on r justifies treating the monopole electric field, $-\partial A_0/\partial\zeta$, as independent of r in the tracking analysis.

Similarly, the relaxation length of the dipole potential A_1 can be determined from Eq. (27), and for self-similar Bennett profiles is given by

$$\zeta_{m1} = (1-\bar{q}) \frac{\pi\bar{\sigma}(0,\zeta)r_b^2}{2c} . \qquad (30)$$

This equation was first derived by Slinker et al.[15] in studies of hose instability. According to Eqs. (28) and (30), the dipole decay length ζ_{m1} is roughly an order of magnitude smaller than the monopole decay length ζ_{mo}. Neglecting the dipole electric field, $-\partial A_1/\partial\zeta$, relative to the monopole field, $-\partial A_0/\partial\zeta$, is thus well justified in the tracking analysis. We state without proof that the dipole field acts to reduce the channel

14

force, and that the linearized tracking result (10) can be recovered from Eq. (27) by dropping $\partial A_1/\partial \zeta$ and using the fact that the local magnetic deflection force equals $-e\underline{\nabla}_\perp A$.

B. Longitudinal Coupling and the Resistive Hose Instability

The channel tracking force calculated in the previous sections varies with distance ζ into the pulse. As the beam bends in response to this force, it perturbs the electromagnetic fields. The plasma retards the growth and decay of these perturbations and thus generates a longitudinal coupling force, as the fields produced by early beam segments persist to guide later segments. Although a detailed analysis of dynamical effects is beyond the scope of this paper, the importance of coupling, both to tracking and to the resistive hose stability, warrants a brief discussion. Further discussion of coupling is given in the Appendix.

Coupling develops from dipole electric fields that are short-lived ($\zeta_{m1} \ll \zeta_{mo}$) relative to the monopole fields responsible for channel tracking. As a consequence, the channel force exceeds the coupling force as long as the channel offset and size remain modest, $y_c < r_c \sim r_b$, and as long as the simple chemistry model discussed earlier remains valid. As discussed in Sec. V-A, however, the latter assumption fails at late ζ, as higher-order chemistry causes the channel force to change sign and repel the beam. The beam tail would then be ejected from the channel, even though the head tracks, in the absence of coupling.

Although coupling is relatively unimportant early in the beam head, it becomes important in the body where cumulative ionization produces a large dipole decay length ζ_{m1}. If the channel force changes sign quickly over ζ_{m1}, the coupling force will dominate and cause subsequent portions of the

beam to follow the head, regardless of the channel force. Coupling can thus keep the entire beam in the channel, provided the channel force is tracking initially and does not become detracking until ζ_{m1} is large.

Although coupling keeps the beam together, it also drives the resistive hose instability, as field perturbations become out of phase with beam oscillations.[14,16] Because the phase lag and growth rate of this instability are governed by the magnetic dipole decay length ζ_{m1}, slow changes in the channel force over ζ_{m1} should not excite strong hose growth. To the contrary, a channel force that is tracking and stronger than the coupling force should reduce hose growth by providing a fixed central axis of attraction. Because hose is a convective instability and because ζ_{m1} rises with ζ, damping is most important in the beam head[16] which is where density tracking is strongest. Density tracking can thus suppress the hose instability, as well as keep the beam in the channel.

C. Electrostatic Forces

The preceding magnetic tracking analysis is restricted to the high-conductivity region where the electrostatic fields and forces are small. The electrostatic fields are not small, however, early in the beam head where the conductivity is low. Nevertheless, several effects conspire to reduce the impact of these fields on beam steering.

Electrostatic deflection forces arise as the channel conductivity asymmetrically neutralizes the electrostatic field of the beam, thereby polarizing the plasma charge. Because deflection develops from charge polarization rather than from a unipolar charge, the deflection force varies with radius r, and hence its average value is small.

16

A second mitigating effect is that the plasma charge polarizes on a monopole decay length given by

$$\zeta_{eo} = c/4\pi\sigma, \tag{31a}$$

but relaxes on a dipole decay length given by

$$\zeta_{e1} = c/(1-\bar{q})2\pi\sigma. \tag{31b}$$

These relationships can be derived using charge conservation and Gauss's law.[8] Because the two lengths are comparable, electrostatic deflection decays nearly as rapidly as it arises, thus reducing its peak value. By contrast, magnetic deflection attains full value because it decays slowly relative to its growth, $\zeta_{mo} \gg \zeta_{m1}$.

A third limitation is the rapid growth of σ from beam ionization. This ionization quickly reduces ζ_{e1}, thereby confining electrostatic deflection to near the beam head. Because longitudinal coupling is not well developed there, electrostatic deflection is ineffectual at steering the beam, as well as weak.

V. GAS CHEMISTRY

A. Plasma-Electron Collision Frequency

The chemistry parameter q (or $\bar{q}$) determines the sign and magnitude of the channel force, and it thus largely determines the behavior of beams in density channels in a given gas. In this section, we discuss the physical

basis for q and ν_{mo}, and determine their dependence on gas chemistry and beam heating.

As noted earlier, the reduced collision frequency ν_m in a weakly ionized gas equals an average of the plasma electron speed times the cross section for momentum transfer to the gas molecules. The average electron speed increases as the square root of the plasma electron temperature T_e, and for most gases this dependence causes ν_m to rise with T_e. If ν_m rises with T_e, and if T_e falls with gas density N, the parameter q in Eq. (6) is positive, and the channel force is tracking. Otherwise, the force is detracking.

The dependence of T_e on N can be determined as follows. The plasma electrons gain energy from both ohmic heating and direct beam heating, and lose energy via collisions with the gas molecules. Ohmic heating derives from the electric fields of the beam and plasma, while direct beam heating is a by-product of beam impact ionization. Setting the cooling rate of the plasma electrons equal to their heating rate yields

$$nN\nu_c = \sigma E^2 + f_h \, (j_b/e) \, N \, \frac{d\varepsilon}{dx} , \qquad (32a)$$

where ν_c is the reduced inelastic cooling rate for the plasma electrons, $d\varepsilon/dx$ is the reduced energy-loss function for the beam, and f_h is the fraction of deposited beam energy going into heating of the plasma electrons. For a given gas, ν_c is a function of T_e only, and $d\varepsilon/dx$ is a function of beam energy γ only. For relativistic electron beams in air, $d\varepsilon/dx \sim 2\text{-}3$ keV/cm-atm, and $f_h \sim 0.2$.

Equation (32a) can be rewritten by dividing by nN and substituting Eq. (1) for σ. This yields a transcendental equation for the plasma electron temperature T_e:

$$\nu_c(T_e) = \frac{e^2}{m\nu_m(T_e)} \left(\frac{E}{N}\right)^2 + \frac{f_h}{e}\frac{d\varepsilon}{dx}\left(\frac{j_b}{n/N}\right)\frac{1}{N} \cdot \tag{32b}$$

To lowest order, the electric field E and the degree of ionization n/N are independent of gas density N. As a consequence, lowering N raises the heating rate on the right-hand side of Eq. (32b). T_e is thus elevated in regions of low N. The elevation is usually modest, however, because ν_c rises rapidly with T_e for temperatures of interest, $T_e \sim 1$ eV. The weak dependence of T_e on N is responsible for the weak dependence of the tracking force on N.

The chemistry parameter q is determined by Eqs. (6) and (32b) and the dependence of ν_m and ν_c on T_e. A much simpler estimate can be obtained, however, by ignoring direct beam heating relative to ohmic heating. The reduced collision frequency ν_m can then be expressed as a function of E/N, without reference to T_e. The neglect of direct beam heating is usually valid when the beam and its fields are intense.

As an example, we plot in Fig. 3 the reciprocal of ν_m as a function of the reduced field E/N in air. This curve was computed from the electron drift speed, $w = eE/mN\nu_m$, as calculated by Heylen[17] and tabulated by Dutton.[18] For convenience, E/N is normalized to the avalanche air breakdown strength, $E_b/N = 25$ kV/cm-atm. Much above this field, avalanche-induced detracking is likely, as discussed in the next section.

Figure 3 indicates that the chemistry model (18) is a crude but adequate approximation over limited ranges of E/N. In this model, the parameters q and ν_{mo} are weak functions of the electric field $E(\zeta)$, which is assumed to be independent of r. Typical values for air are q $\simeq$ 0.2 and $\nu_{mo} \simeq 10^{-7}$ cm^3/s for 0.1 $E_b/N \leq E/N \leq E_b/N$; at lower fields, q $\simeq$ 0.5.

Replotting ν_m to fit form (25) shows equally good agreement, with $\bar{q} \simeq 0.2$ at high fields and $\bar{q} \simeq 0.5$ at the lower fields. All of these parameters are insensitive to the nature of the heating mechanism, provided the cooling rate ν_c remains a strong function of T_e. The addition of direct beam heating should not, therefore, notably affect q, $\bar{q}$, or ν_{mo}.

B. Other Sources and Sinks of Ionization

Density tracking derives from simple but subtle chemistry properties, and this raises the concern that other processes may be equally important. In this section, we examine the effects of higher-order chemistry on n/N. A more careful numerical analysis was performed by Keeley[19] using a detailed air chemistry code.

The behavior of n/N can be examined using a generalized continuity equation for the plasma electrons:

$$\frac{\partial n}{\partial t} - N s_i j_b/e = (\nu_a - \beta_a)nN - \beta_r n^2 - \nabla \cdot (n\underset{\sim}{v}) , \qquad (33)$$

where s_i is an effective beam ionization cross section, ν_a is an electron avalanche coefficient, β_a is an electron attachment coefficient, β_r is an electron-ion recombination coefficient, and $\underset{\sim}{v}$ is the plasma-electron fluid velocity. In the preceding analysis, all terms on the right-hand side of Eq. (33) were neglected. We separately assess each of these terms, using the frozen approximation that $\partial/\partial t = c \, \partial/\partial \zeta$.

The electron avalanche coefficient ν_a is a strong function of E/N, and thus it preferentially produces high n/N and high σ in a low-density channel. High channel conductivity _increases_ the plasma return current in the channel, which repels the beam. Avalanching must therefore be kept small relative to beam ionization to keep the net channel force tracking.[11]

This requires high channel gas density N_c and modest electric field E. A generally sufficient condition is

$$E/N_c \lesssim 3(E_b/N), \tag{34}$$

where E_b/N is the minimum reduced field needed to initiate avalanching. Condition (34) bounds the minimum channel depth for a given beam.

The effect of electron attachment, which converts free electrons to essentially immobile negative ions, depends on the dependence of the attachment coefficient β_a on temperature T_e and gas density N. If there is little or no temperature dependence, the effect is detracking, because attachment lowers n/N more outside the density channel than inside, so that plasma return current flows preferentially in the channel. This detracking becomes important at distances

$$\zeta \gtrsim c/\beta_a N_o \tag{35}$$

from the head.

Electron-ion recombination is detracking for the same reason. Namely, it lowers n/N more outside the channel than in. Recombination becomes important at

$$\zeta \gtrsim c\sqrt{e/\beta_r s_i N j_b} , \tag{36}$$

where $N j_b$ is to be evaluated at its maximum value.

C. Plasma Dynamic Effects

In addition to the chemistry issues, the analysis neglects several plasma dynamic effects. One of these is plasma electron convection represented by the last term in Eq. (33). Convection perturbs n/N much like a source or sink of ionization, but can usually be neglected because the electron fluid velocity is typically small,

$$w/c \lesssim 10^{-3}. \tag{37}$$

A related dynamical effect is electron pressure in Ohm's law. Electron pressure can be neglected provided

$$T_e \ll eEr_b, \tag{38}$$

which is usually well satisfied except for very narrow beams.

A third dynamical effect is the finite time taken for plasma heating. This time can be neglected provided the beam parameters vary slowly. A sufficient condition, based on ohmic heating alone, is

$$c \frac{\partial}{\partial \zeta} \ll eEw/T_e. \tag{39}$$

The heating time for intense beams in air is typically sub-nanosecond.

A fourth effect is diffusion from beam ionization. Beam ionization liberates energetic secondaries that produce additional ionization through a cascade process. The total ionization is thus spread in space and time inversely proportional to N.[20,21] This spread preferentially reduces the formation rate of σ in the low-density channel, an effect that should enhance tracking.

A fifth neglected effect is momentum transfer between the plasma electrons and ions. These Spitzer collisions become important at high degrees of ionization, $n/N \gtrsim 10^{-2}$, and cause ν_m to decrease rather than increase with T_e, thereby producing detracking. In initially un-ionized gases, however, n/N is initially small, and hence collisions with ions are usually negligible in the beam head where tracking is most important.

D. Channel Preionization

The assumption that the channel is un-ionized prior to beam injection fails if the channel is deep and in thermodynamic equilibrium. In equilibrium, a deep channel must be hot to maintain pressure balance with the background gas, and hence it must be thermally ionized. Return currents induced in this ionization can eject the beam.[7] In this section we determine how much preionization can be tolerated, and the limitations that thermal preionization imposes on channel depth.

Channel preionization produces magnetic and electrostatic deflection forces. As discussed earlier, the magnetic forces develop on the dipole decay length ζ_{m1} and relax on the monopole decay length ζ_{mo}, while the electrostatic forces develop on the monopole decay length ζ_{eo} and relax on the dipole decay length ζ_{e1}. All the forces relax more slowly than they develop.

At low levels of preionization, ζ_{e1} initially exceeds ζ_{mo}, and thus the electrostatic forces initially dominate. These forces are relatively ineffectual, however, at steering the beam as discussed in Sec. IV-C.

By contrast, at high levels of preionization, ζ_{m1} everywhere exceeds ζ_{e1}, and the magnetic forces then dominate everywhere. According to Eqs. (30) and (31), ζ_{m1} exceeds ζ_{e1} for all ζ provided

$$(1-\bar{q})\pi\sigma_i r_b/c \geq 1, \tag{40}$$

where

$$\sigma_i = \frac{e^2 n_i}{mN\nu_m} \tag{41}$$

is the conductivity resulting from the channel preionization, n_i. Yu[22] derived a variation of condition (40) and termed it the channel overheat condition to signify the onset of strong magnetic detracking.

In a density channel, account must be taken of the density force F_{tm}. To avoid repetition, we will not compute the detracking force from channel preionization, but instead determine only when it is cancelled by F_{tm}.

For simplicity, consider a square density channel of radius r_c that is uniformly preionized and entirely inside a square beam of radius $r_b > r_c$. Assuming beam impact ionization only, the uniform channel preionization, n_i/N, is supplemented by uniform beam ionization, $n(\zeta)/N$. The gas-density depression then perturbs the plasma current by an amount proportional to the change in ν_m,

$$\delta j_d = \frac{e}{m} E_z \left(\frac{n}{N}\right) \left[\frac{1}{\nu_m(N)} - \frac{1}{\nu_m(N_o)}\right], \tag{42}$$

while the channel preionization perturbs the plasma current by

$$\delta j_i = \frac{e}{m} E_z \left(\frac{n_i}{N}\right) \frac{1}{\nu_m(N)}. \tag{43}$$

The current δj_d produces tracking while δj_i produces detracking.

Because the two currents have the same spatial distribution, the net magnetic channel force equals zero when they cancel, $\delta j_i + \delta j_d = 0$. The transition from detracking to tracking thus occurs at the point ζ_t where

$$n(\zeta_t) = n_i \left[\frac{\nu_m(N_o)}{\nu_m(N) - \nu_m(N_o)} \right]$$

$$= n_i \frac{1 - q \ln(N_o/N)}{q \ln(N_o/N)} \tag{44a}$$

$$= n_i \left[\left(\frac{N_o}{N} \right)^{\bar{q}} - 1 \right]^{-1}. \tag{44b}$$

Form (44a) is based on chemistry relationship (18) for ν_m, while form (44b) is based on chemistry relationship (25). For deep channels, the force typically transitions from detracking to tracking once $n(\zeta) > n_i$.

As discussed earlier, the magnetic coupling force relaxes on the dipole decay length ζ_{m1}. Coupling is thus strong at ζ_t provided

$$(1-\bar{q}) \pi \sigma_i r_b^2/c \gtrsim \zeta_t. \tag{45}$$

This condition is stronger than the channel overheat condition (40), provided $\zeta_t > r_b$. The latter proviso is in fact fundamental to the analysis which presumes that the beam and plasma vary slowly, $r_b \, \partial/\partial\zeta \ll 1$. The proviso fails only for extremely intense beams, for which displacement currents and like effects must be incorporated.

For beams of interest, condition (45) is sufficient and generally necessary for channel preionization to eject the entire beam. The head is ejected because the net channel force is detracking, while the body is

25

ejected because it is coupled to the head. If condition (45) is not satisfied, the detracking portion of the head is still ejected, but later portions of the beam can track the channel. As discussed in the Appendix, detracking condition (45) is imprecise because it does not account for the different parametric dependencies of the channel and coupling forces. The Appendix also shows that condition (45) can be difficult to meet.

Although conditions (40) and (45) differ significantly regarding n_i/N, the difference is often insignificant regarding allowed channel depth. This is because n_i/N is a strong function of N for a thermalized but weakly ionized gas in pressure balance. To show this, consider the Saha equation which states that the degree of thermal preionization n_i/N in a weakly ionized gas is proportional to $\exp(-W_i/2T_g)$, where W_i is the gas ionization potential and T_g is the local gas temperature.[23] The gas is weakly ionized only if $T_g \ll W_i/2$, in which case n_i/N is a very strong function of T_g. In pressure balance, the gas density varies inversely with temperature, $N \propto T_g^{-1}$, so that n_i/N varies strongly with N. For example, halving the channel gas density at fixed pressure raises n_i/N by over six orders of magnitude at temperatures $T_g \lesssim W_i/30$. This strong variation usually causes detracking condition (45) to be satisfied at channel temperatures much above $W_i/30$. In hot air, for example, the lowest ionization potential is $W_i = 9.3$ eV for NO, so that condition (45) is usually satisfied if the channel temperature rises much above 0.3 eV. This temperature restriction limits the depth of the channel, and thus limits the degree of beam-range extension possible.

E. Chemistry Summary

The preceding analysis of gas chemistry suggests that the beam head is likely to track the channel, as long as channel preionization and on-axis avalanching are weak or absent. Although the beam body may experience detracking from higher-order chemistry, longitudinal coupling causes the body to follow the head. The sign and magnitude of the channel force is thus most important in the region where coupling first dominates.

As discussed in Sec. V-B, we have verified the change in sign of the tracking force at late ζ, as a function of various chemistry processes. More exact chemistry analysis by Keeley[19] shows qualitatively similar results. We have also performed dynamical simulations, to be reported in a later paper, showing that the entire beam can be pulled into the channel, even when the channel force is detracking in the body. The first such simulation was performed by Welch[11] using the particle code IPROP. The dynamical codes employ relatively simple chemistry, and they initially failed to detect density tracking because ν_m was taken to be constant.

VI. STATIC SIMULATIONS

A. Comparison with Analytic Theory

We have used two computer codes, VIPER[16] and SARLAC,[24] to compute the average force produced by a density channel on a rigid-rod beam. For this purpose, the beam is not propagated in z but is treated as frozen. In dynamical runs, which will be described in a later paper, the beam is allowed to move, although Maxwell's equations are still solved using the frozen approximation, $d/dz = 0$. VIPER is a linearized code limited to small beam displacements, while SARLAC is a nonlinear particle code.

To test the nonlinear theory, SARLAC was run using beam impact ionization only, a density channel given by Eq. (14), and a collision frequency given by

$$\nu_m(r,\theta,\zeta) = \frac{\nu_{mo}}{1 - q \ln[(E/N)/(E_o/N_o)]} , \qquad (46a)$$

where E is the total electric field and q, ν_{mo}, and E_o/N_o are constants. The form of this equation requires a normalization coefficient given by

$$k(\delta) = 1 + \frac{pq}{2} \left[\ln(\delta) + g_1(1) - g_1(\delta)\right] - q \ln\left(\frac{E'/N}{E_o/N_o}\right) , \qquad (46b)$$

in place of Eq. (20d). Here E' equals I_p divided by the plasma conductance. In the results presented below, E' was set for convenience to the on-axis electric field strength.

Simulations were performed using a beam with a Bennett profile of constant radius r_b = 1 cm and a current I_b that rose linearly to 10 kA in 10 ns and then remained constant. The parameters δ, p, y_c, r_c, q, ν_{mo}, and E_o/N_o were varied over more than an order of magnitude. In Fig. 4 we plot the net deflection force, $F_t(\zeta)$, as computed by SARLAC for several typical runs. This force, which includes contributions from the plasma charges and displacement currents, agrees well with the magnetic channel force, $F_{tm}(\zeta)$ given by the theory, after a few ns. Observe that the peak tracking force, 6 Gauss in Fig. 4a, is roughly two orders of magnitude smaller than the monopole pinch force at that point in the beam. Beam distortion should therefore be negligible. The detracking exhibited at early ζ is an electrostatic artifact of SARLAC, and is not seen in VIPER (or in SARLAC if the beam head is flared.) Dynamical runs, to be described in a later paper, show the beam being pulled into the channel after propagating a distance consistent with Eq. (12).

28

B. Gas Chemistry

To examine the effects of various chemistry processes on channel tracking, we performed a series of runs using the linearized code VIPER. In these runs, the beam current rose smoothly from zero to 20 kA, and the beam radius fell smoothly from 2.65 cm to 1 cm, over a time scale of 10 ns ($\Delta\zeta$ = 300 cm). The radius variation approximates the flaring that develops naturally from weak pinching of the beam head.[25] A Bennett profile was used for the beam, and a Bennett profile of radius r_c = 3 cm was used for the channel depth. The ambient gas density was N_o = 1 atm, and the on-axis channel density was N_c = 0.3 atm.

VIPER employs an air chemistry model[26] containing all but the convection term in the continuity equation (33). In Fig. 5 we plot the net channel force as a function of ζ as various chemistry processes are turned on separately and in total. Curve (a) plots F_t/y_c using beam ionization only; the force is everywhere tracking and agrees well with the analytic predictions. Curve (b) adds electron attachment to O_2 at a rate $\alpha_a N_o \sim$ 5×10^7 s^{-1}; attachment weakens the density channel force consistent with Eq. (35), but does not cause actual detracking until much later. Curve (c) shows the effect of electron-ion recombination with a rate coefficient $\beta_r \sim$ 10^{-7} cm^3/s; recombination weakens the density channel force consistent with Eq. (36), but again does not cause detracking until much later. Curve (d) shows the effect of Spitzer collisions which, for the given parameters, degrade detracking more than attachment or recombination. Curve (e) shows the cumulative effect of all these processes. Observe that the channel force remains tracking to $\zeta \geq 600$ cm, well into the region of strong magnetic coupling. The entire beam is thus predicted to track the channel.

Shortening the beam rise time increases the inductive electric field E_z. This raises T_e and ν_m so that the plasma conductivity decreases, until the field is so high that avalanching commences. For the beam described above, VIPER shows avalanche-induced detracking if the beam current rises faster than 30 kA/ns.

Adding channel preionization in excess of the overheat condition (40) produced strong detracking of the beam head in the VIPER runs. Much lower levels of preionization produced weak channel forces that were attractive or repulsive, on average, depending on ζ and on the relative sizes of the beam and channel. Preliminary dynamical simulations suggest, however, that beam expulsion occurs only if the revised overheat condition (45) is met.

VII. CONCLUSION

The analytic and numerical work presented here strengthens the theoretical base for the density tracking force discovered by Welch.[11] Three chemistry properties underlie the effect. First, beam impact ionization is the dominant source of ionization, and it produces a degree of ionization that is symmetric about the beam. Second, the low-density channel reduces the collisional cooling rate of the plasma electrons, thus raising their temperature. And third, in most gases, the elevated temperature raises the momentum-transfer collision frequency of the plasma electrons, thereby lowering the plasma conductivity. The reduced conductivity lowers the plasma return current in the channel, so that the beam is magnetically attracted to the channel.

Several properties of density tracking make it unusually effective at steering a beam. First, the density-channel force is strong, potentially

30

as strong as the radial pinch force that binds the beam together. Second, the density force is long-lived, because it develops from beam ionization and from magnetic monopole fields, rather than from magnetic dipole or electrostatic fields. Third, the density force transitions smoothly to a longitudinal coupling force that causes the beam body to follow the head, regardless of the sign of the channel force in the body. Fourth, the channel force is tracking in the beam head over a wide parameter range, and remains tracking even as the beam pinches to a narrow radius. This trait is especially important for beams that are radius-tailored[27] to reduce the growth rate of the resistive hose instability. Fifth, the density force helps stabilize the hose instability, particularly in the beam head where stabilization is most needed. And sixth, density tracking develops naturally out of the need to achieve range extension. The principal requirements for density tracking to occur are low channel preionization, weak on-axis avalanching, and a chemistry parameter q that is positive.

In short, density tracking should be capable, under appropriate conditions, of keeping a stable, relativistic electron beam inside a rarefied gas channel. Experiments[11-13] designed to test the theoretical predictions have verified the existence of a robust density-tracking force, although they have not yet demonstrated range extension or clear evidence of longitudinal coupling. The latter issues require longer propagation distances and more stable beams.

ACKNOWLEDGEMENTS

Appendix: Longitudinal Coupling

Longitudinal coupling arises when the beam and local pinch force are misaligned. The misalignment produces a transverse restoring force, denoted the coupling force, on the beam. For small misalignments, the coupling force can be computed by linearizing the pinch force about the beam axis. For a self-similar beam in the magnetic regime, the coupling force takes the form

$$F_c \simeq \frac{eI_n}{r_b c} \frac{y_b - y_n}{r_b} , \qquad (A1)$$

where I_n is the net current, y_n is its centroid, y_b is the beam centroid (replacing y_c in the earlier analysis), and $eI_n/r_b c$ is the average magnetic pinch force. Here we assume $y_b, y_n \ll r_b$ where y_b and y_c are measured with respect to a fixed (density-channel) axis. In addition, I_n is taken to be symmetric about its centroid y_n, and azimuthal asymmetries from a channel are treated separately as a channel force.

We previously found that the magnetic dipole fields responsible for magnetic coupling relax on a dipole decay length ζ_{m1}. This suggests that the net current centroid centers about the beam according to

$$\frac{\partial y_n}{\partial \zeta} \simeq \frac{y_b - y_n}{\zeta_{m1}} . \qquad (A2)$$

Combining Eqs. (A1) and (A2) yields the approximation

$$F_c \propto \frac{eI_n}{r_b c} \frac{\zeta_{m1}}{r_b} \frac{\partial y_n}{\partial \zeta} . \qquad (A3)$$

A dynamical equation for $\partial y_b / \partial z$ closes the problem.[14,16]

33

To calculate the channel force, we had assumed a rigid-rod beam parallel to the channel. We could then ignore the coupling force F_c, because there was no tilt to either the beam or net current, $\partial y_b/\partial\zeta = \partial y_n/\partial\zeta = 0 = y_b - y_n$. However, a channel force that varies with ζ soon causes the beam to separate from the net current and to tilt, so that $y_n \neq y_b$, $\partial y_n/\partial\zeta \neq 0$, and $F_c \neq 0$. A large beam tilt, combined with large ζ_{m1}, can produce a coupling force larger than the channel force. In the beam body, ζ_{m1} is large, and coupling usually dominates so that the body follows the head.

The precise point at which coupling dominates a given channel force is complicated by the different dependencies of the forces on the beam and channel parameters. However, for a channel force that transitions from detracking to tracking or vice versa, the coupling force is likely to dominate provided the transition occurs quickly relative to ζ_{m1}. In the case of channel preionization, condition (45) should be sufficient for coupling to occur.

An interesting observation is that condition (45) can be met only at high beam currents. To show this, let us use the left-hand side of the continuity equation (33) to obtain the general expression

$$\zeta_t \gtrsim ec\pi r_b^2 n(\zeta_t)/N s_i I_b(\zeta_t), \tag{A4}$$

depending on how fast I_b rises with ζ. If we now set $n(\zeta_t) \simeq n_i$, based on Eq. (44), we find that condition (45) can be rewritten as

$$I_b(\zeta_t) \gtrsim \frac{mc^3}{e} \frac{\nu_m(N)}{(1-\bar{q})s_i c} \simeq 17 \text{ kA } \frac{\nu_m(N)}{(1-\bar{q})s_i c}. \tag{A5}$$

34

Typical values in air are $\nu_m \simeq 10^{-7}$ cm^3/s, $\bar{q} \simeq 0.2$, and $s_i \simeq 3 \times 10^{-18}$ cm^2, suggesting that condition (45) is satisfied only for $I_b(\zeta_t) \gtrsim 25$ kA. If the beam current never rises to this value, coupling requirement (45) is never satisfied, and the beam body need not follow the head but is free to track the channel. In principle, then, the body of modest-current beams can track a density channel, regardless of preionization level.

In practice, however, high levels of preionization push ζ_t into regions where higher-order chemistry causes the density force to become detracking. The net channel force is then everywhere detracking, so that coupling is irrelevant, and the entire beam is ejected from the channel. Furthermore, high channel preionization will excite violent hose instability.[16]

References

1. E. P. Lee, Phys. Fluids 19, 60 (1976).

2. R. C. Smith and B. W. Schumacher, Nucl. Instrum. Methods 118, 73 (1974).

3. J. F. Lowry, J. H. Fink and B. W. Schumacher, J. Appl. Phys. 47, 95 (1976).

4. G. Bekefi, B. T. Feld, J. Parmentola and K. Tsipis, Nature 284, 219 (1980).

5. P. A. Miller, R. I. Butler, M. Cowan, J. R. Freeman, J. W. Poukey, T. P. Wright and G. Yonas, Phys. Rev. Lett. 39, 92 (1977).

6. P. F. Ottinger and D. Mosher, Phys. Fluids 22, 332 (1979)

7. D. P. Murphy, M. Raleigh, R. e. Pechacek and J. R. Greig, Phys. Fluids 30, 232 (1987).

8. E. P. Lee, "Calculation of a Tracking Force," Lawrence Livermore National Laboratory Report UCID-19674, January 1983, unpublished.

9. B. Hui and M. Lampe, J. Comp. Phys. 55, 328 (1984). See also B. Hui and M. Lampe, "Numerical and Analytical Studies of Beam Channel Tracking," Naval Research Laboratory Memo Report 5136, ADA139148 (1984).

10. J. A. Masamitsu, S. S. Yu and F. W. Chambers, "Beam Tracking Studies with RINGBEARER II," Lawrence Livermore National Laboratory Report UCID-19674, November 1982, unpublished.

11. D. R. Welch, F. M. Bieniosek and B. B. Godfrey, Phys. Rev. Lett. 65, 3128 (1990).

12. D. P. Murphy, R. E. Pechacek, D. P. Taggart and R. A. Meger, "Density Channel Tracking Studies on Pulserad," Naval Research Laboratory Memo Report 6770 (1991).

13. D. P Murphy, R. E. Pechacek, T. A. Peyser, J. A. Antoniades, M. C. Meyers, J. Santos and R. A. Meger, Bull. Am. Phys. Soc. 35, 2071 (1990).

14. E. P. Lee, Phys. Fluids 21, 1327 (1978).

15. S. P. Slinker, R. F. Hubbard and M. Lampe, J. Appl. Phys. 62, 1171 (1987).

16. M. Lampe, W. Sharp, R. F. Hubbard, E. P. Lee and R. J. Briggs, Phys. Fluids 27, 2921 (1984).

17. A. E. D. Heylen, Proc. Phys. Soc. (London) 79, 284 (1962).

18. J. Dutton, J. Phys. Chem. Ref. Data 4, 577 (1975).

19. D. A. Keeley, private communication.

20. S. P. Slinker, A. W. Ali and R. D. Taylor, J. Appl. Phys. 67, 679 (1990).

21. M. J. Berger, S. M. Seltzer and K. Maeda, J. Atm. Terr. Phys. 36, 591 (1974).

22. S. S. Yu, private communication.

23. See, for example, Y. B. Zel'dovich and Y. P. Raizer, Physics of Shock Waves and High-Temperature Hydrodynamic Phenomena, W. D. Hayes and R. F. Probstein, eds., Vol. I (Academic Press, New York, 1966), p. 195.

24. G. Joyce, R. Hubbard, M. Lampe and S. Slinker, J. Comp. Phys. 81, 193 (1989).

25. W. M. Sharp and M. Lampe, Phys. Fluids 23, 2383 (1980).

26. S. P. Slinker and R. F. Hubbard, "The Viper Conductivity Model," Naval Research Laboratory Memo Report 5777, ADA167134 (1986).

27. M. Lampe, R. F. Fernsler and R. F. Hubbard, Bull. Am. Phys. Soc. 35, 2083 (1990). See also R. F. Hubbard, S. P. Slinker, R. F. Fernsler M. Lampe and G. Joyce, op. cit.
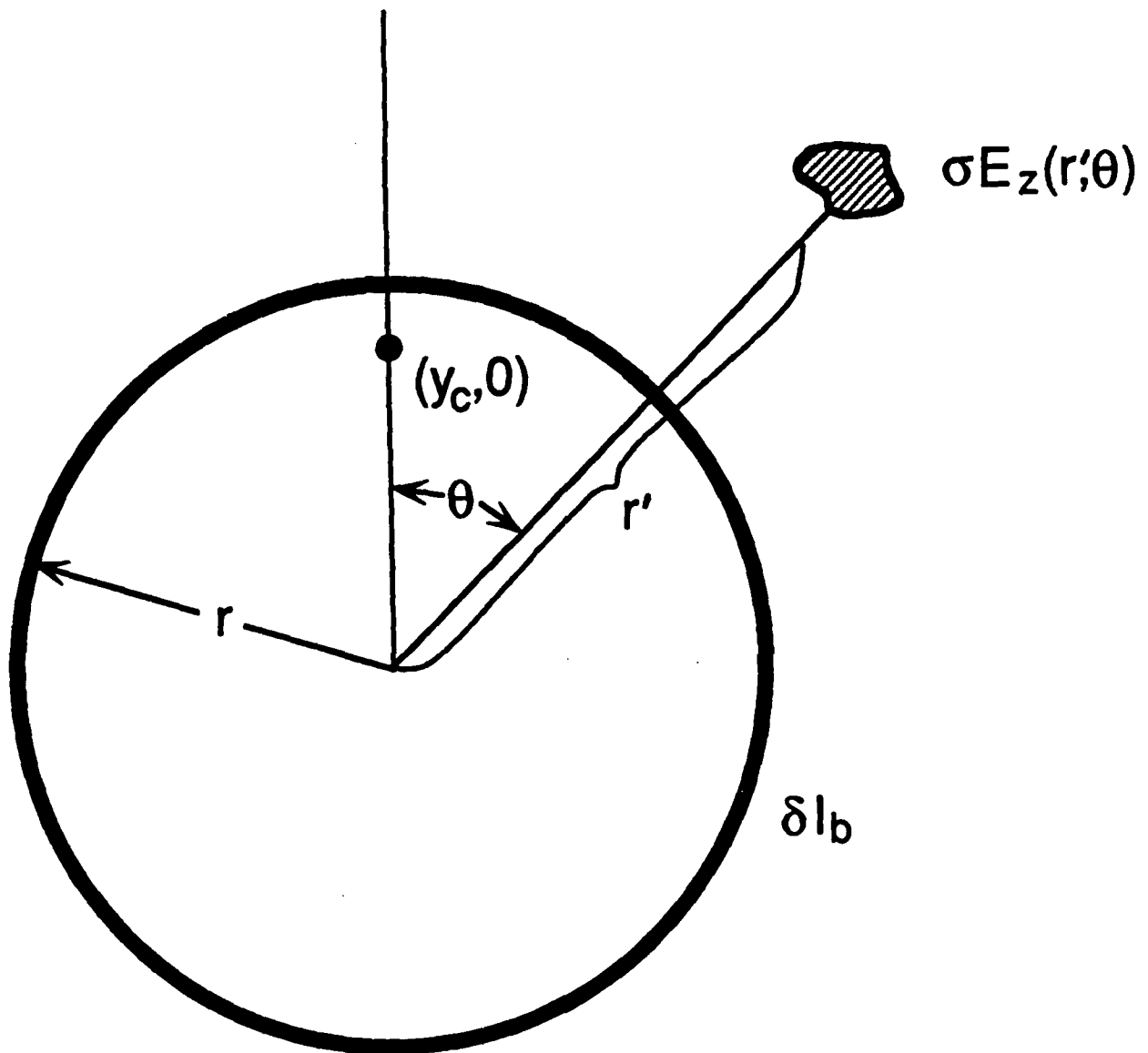
Fig. 1 — An element of plasma current σE_z at (r, θ) deflects a beam ring of radius r. Only currents outside the ring, $r' > r$, deflect it. The direction $\theta = 0$ is defined by the line from the beam centroid $(0,0)$ to the density-channel centroid $(y_c, 0)$.
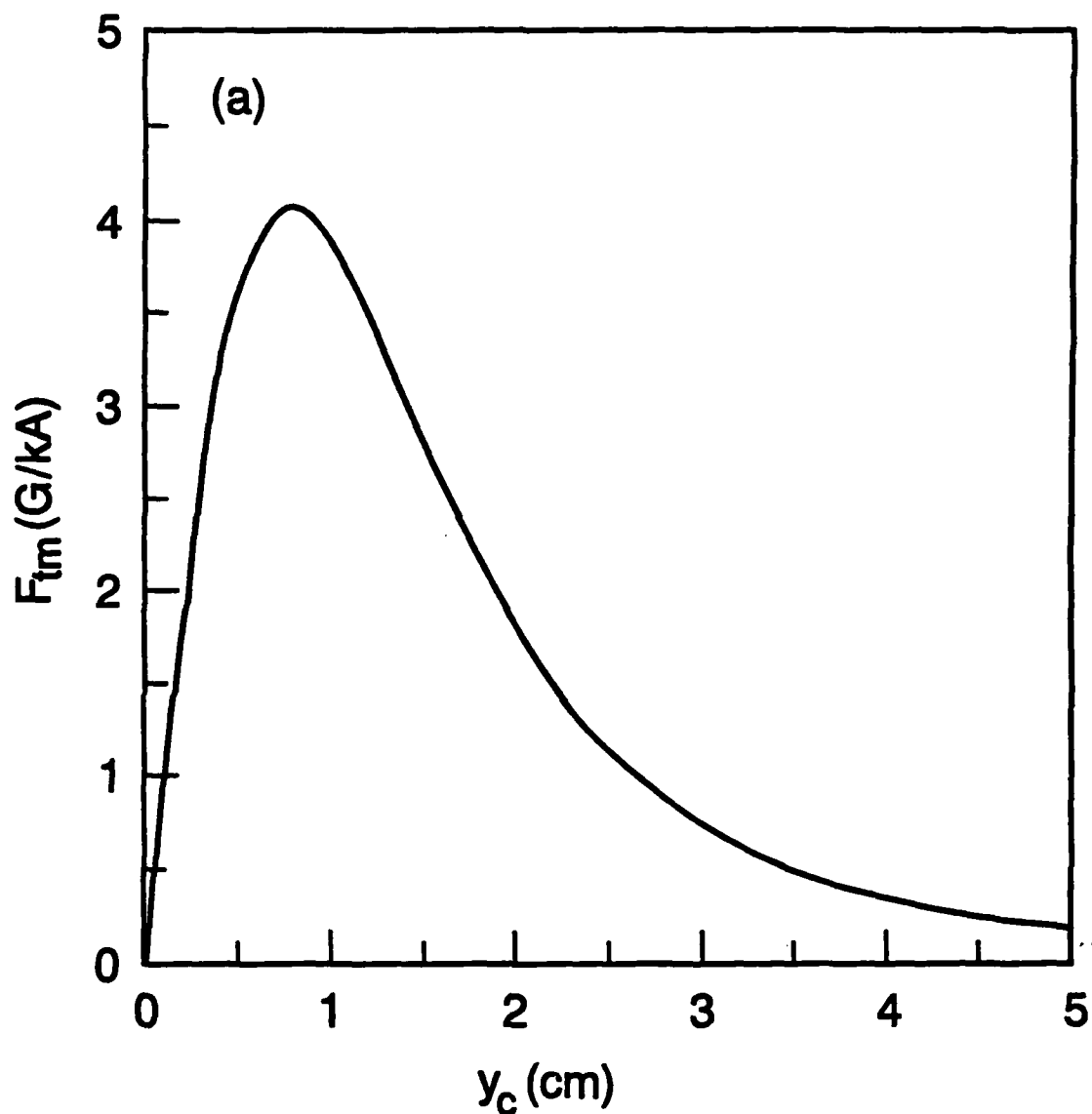
Fig. 2a — Density force $F_{tm}(\int)$ as a function of channel offset y_c. F_{tm} is given in units of Gauss per kA of plasma return current, calculated using Eqs. (19)-(20) with the following nominal parameters: $r_b = r_c = y_c = 1$ cm, $q = 0.2$, $\delta = 0.1$, and $p = 1$.
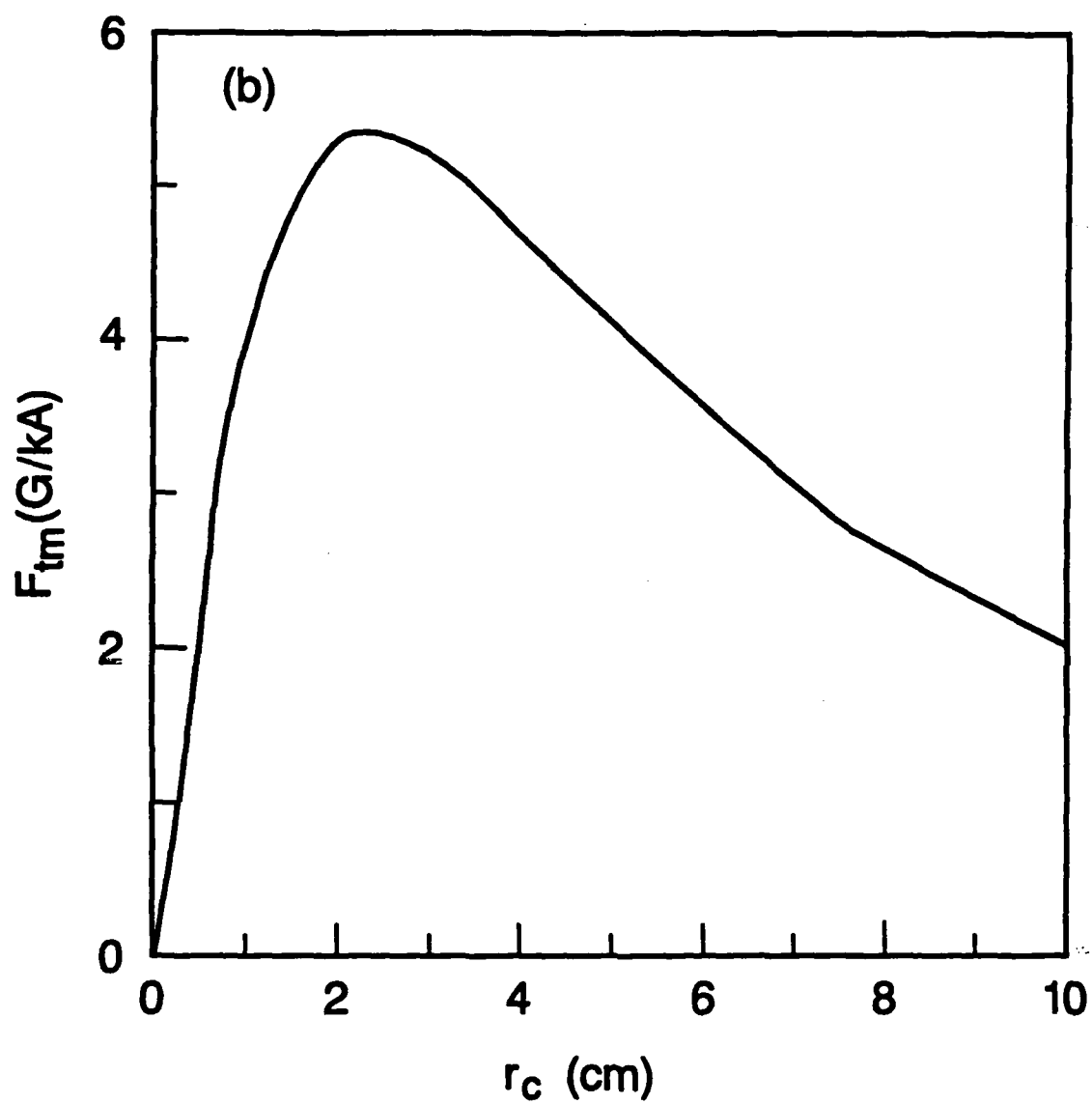
Fig. 2b — Density force $F_{tm}(\zeta)$ as a function of channel radius r_c.

40
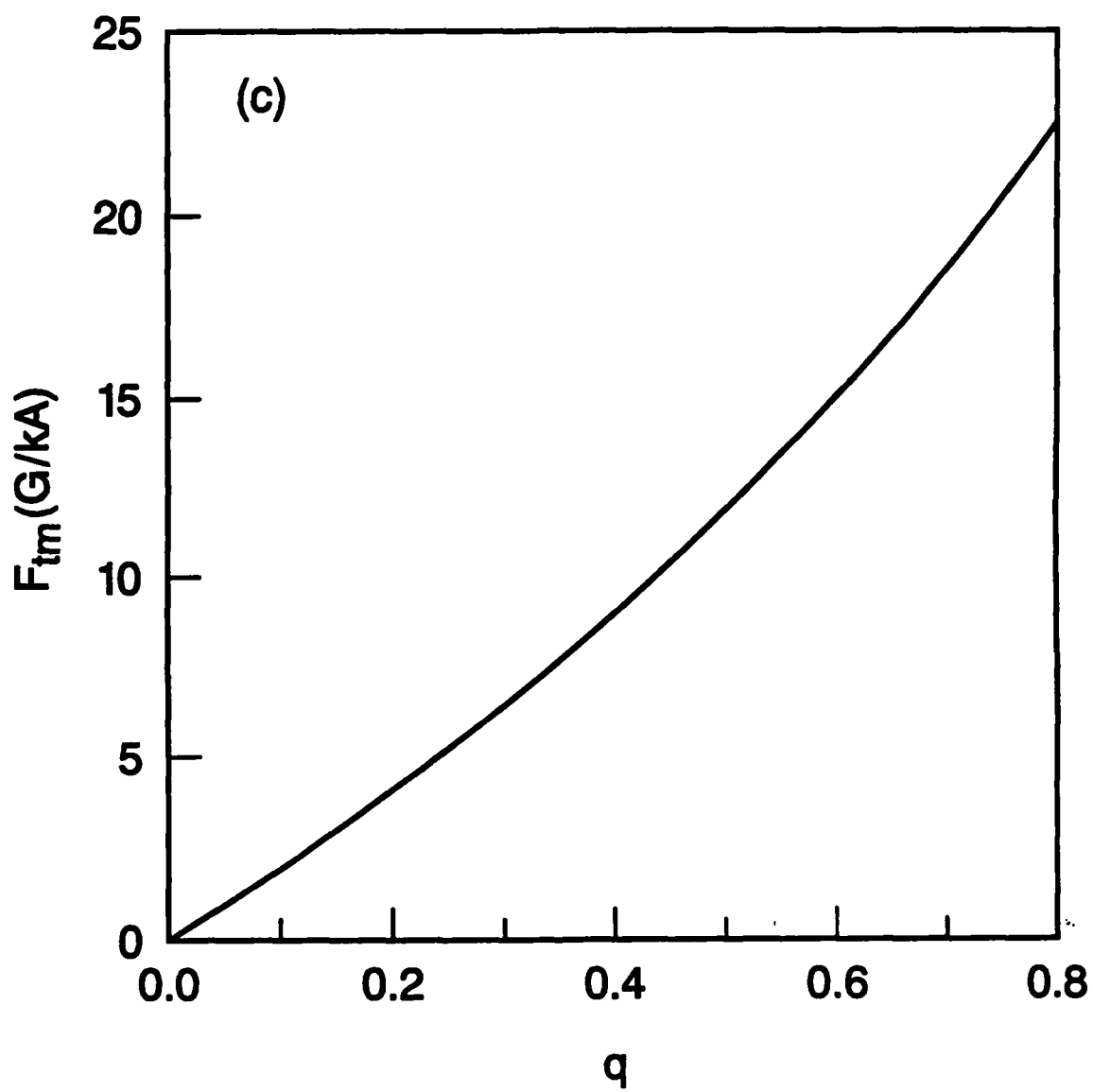
Fig. 2c — Density force $F_{tm}(\zeta)$ as a function of chemistry parameter q.
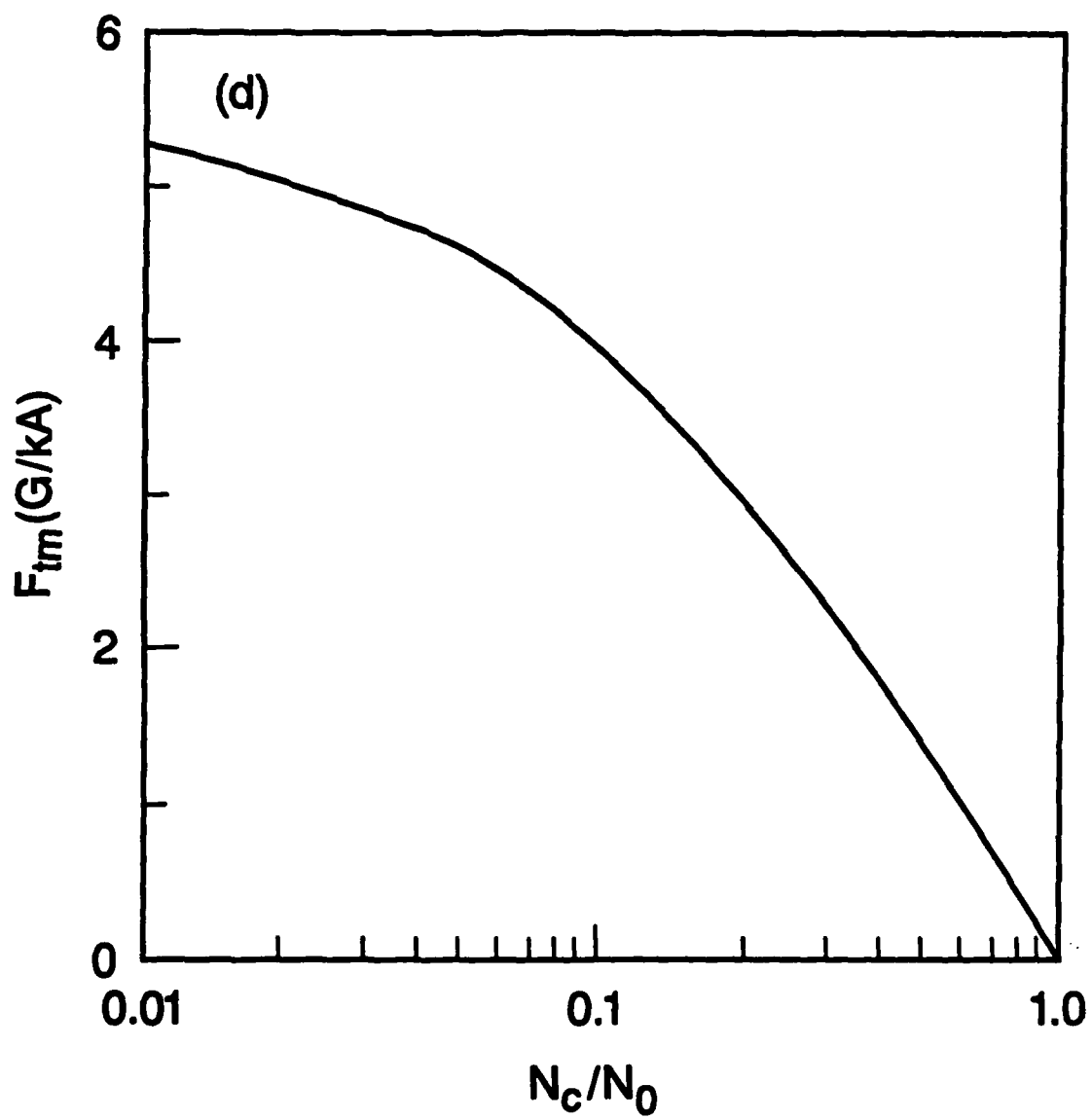
Fig. 2d — Density force $F_{tm}(\zeta)$ as a function of channel depth δ.

42
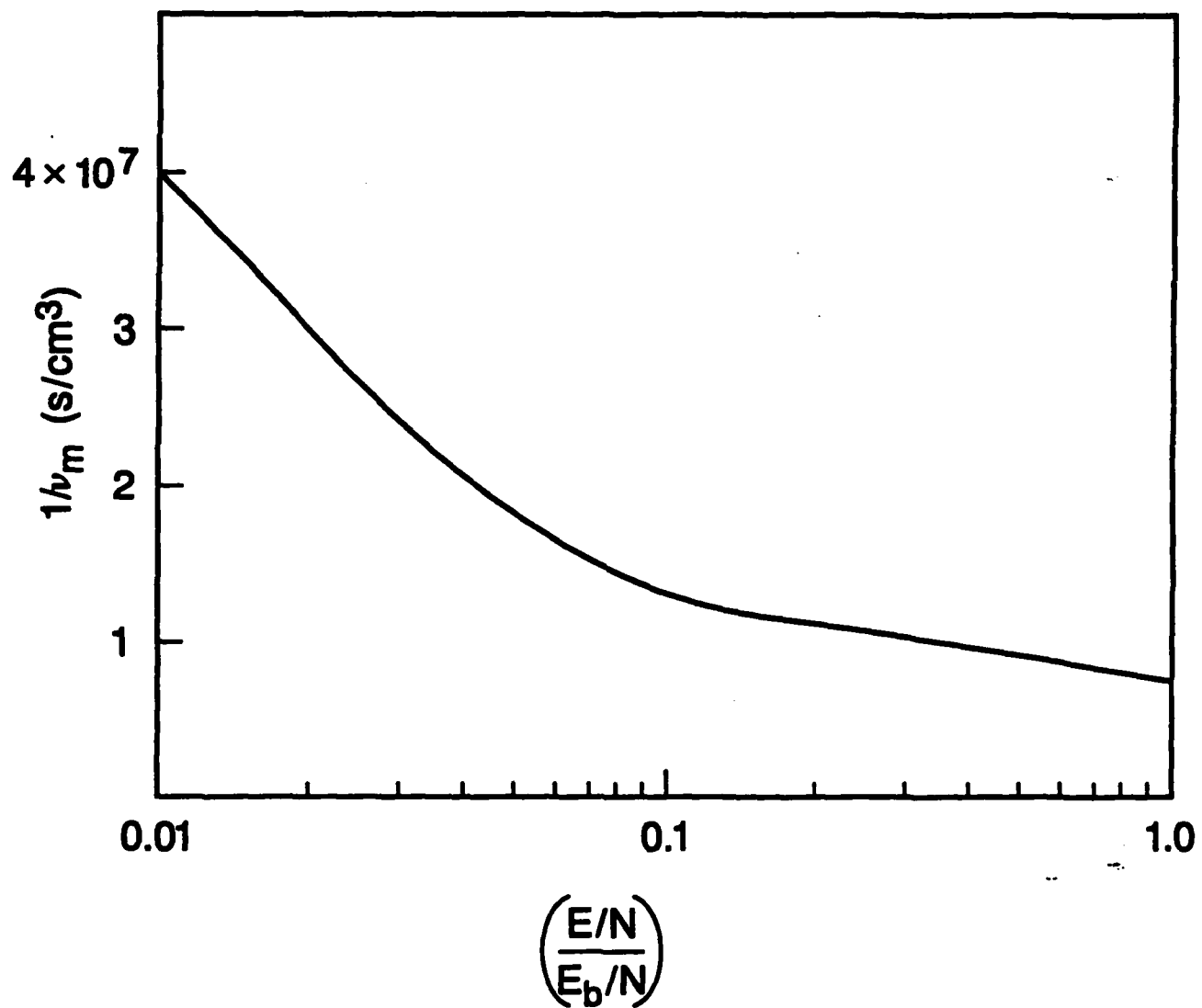
Fig. 3 — The inverse of the reduced collision frequency ν_m as a function of electric field in air.
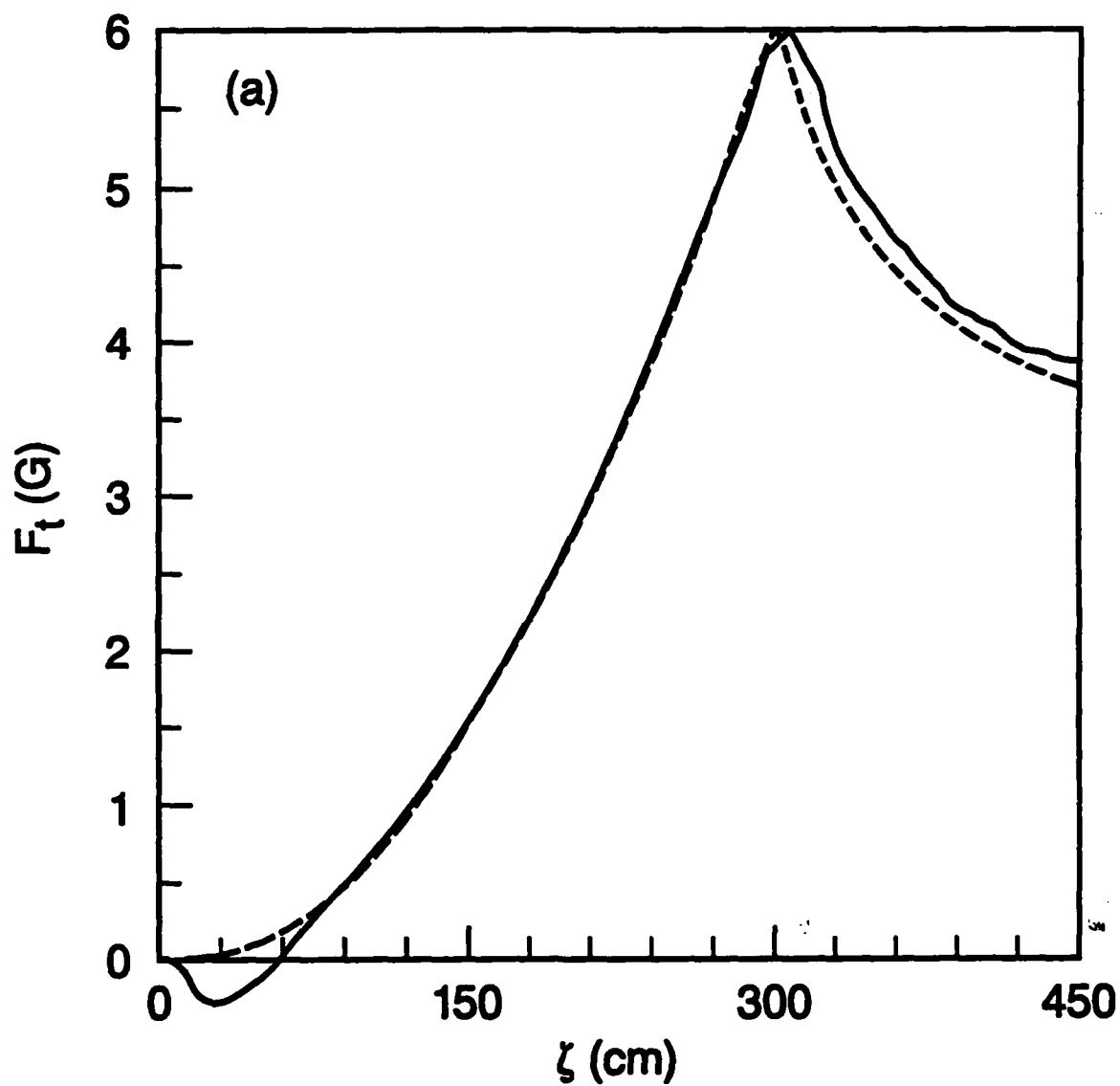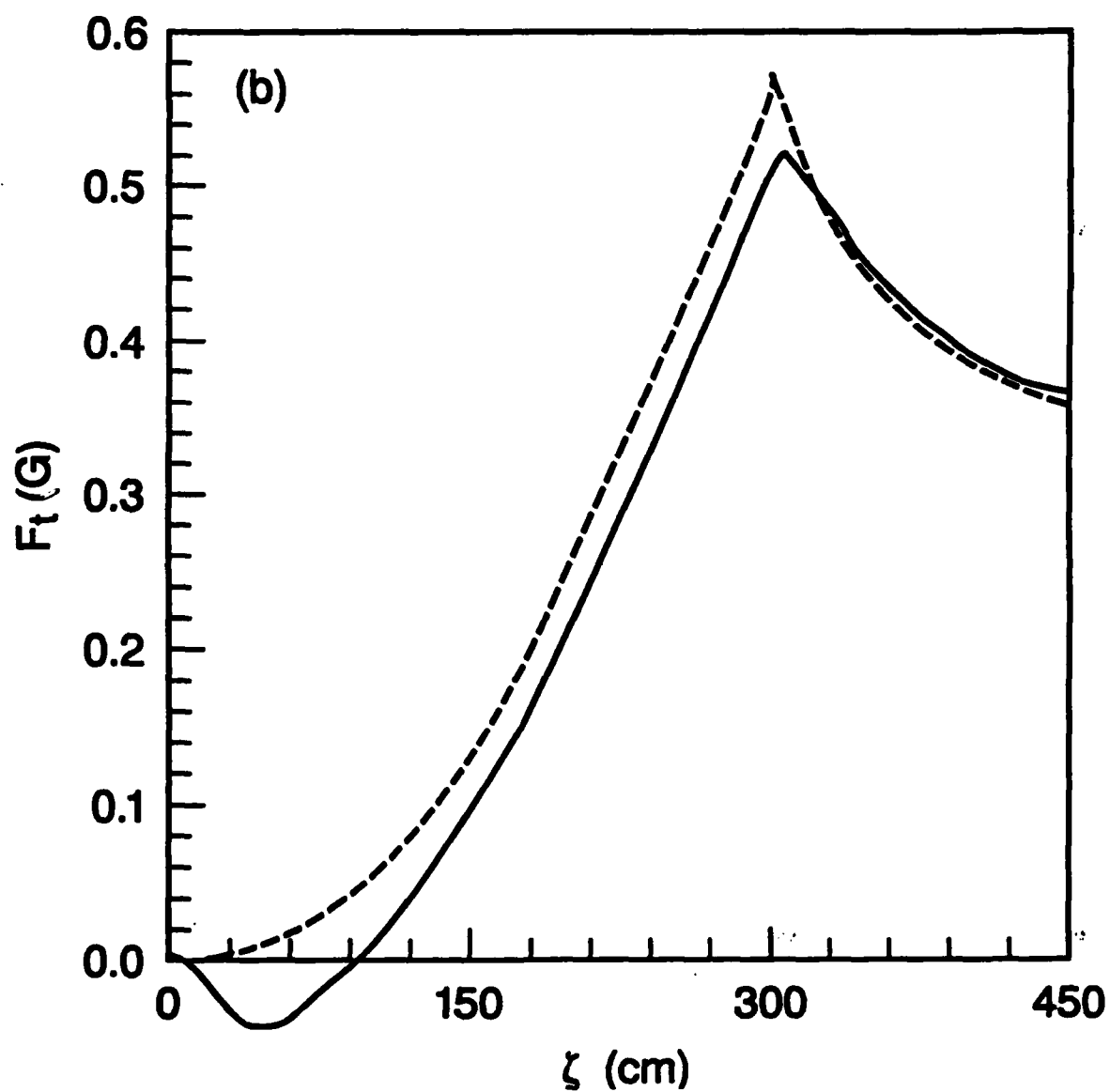
Fig. 4a — Typical comparison plots of the total numerical tracking force F_t [solid line] and the theoretical magnetic force F_{tm} [dashed line] for $y_c = 1$, $r_c 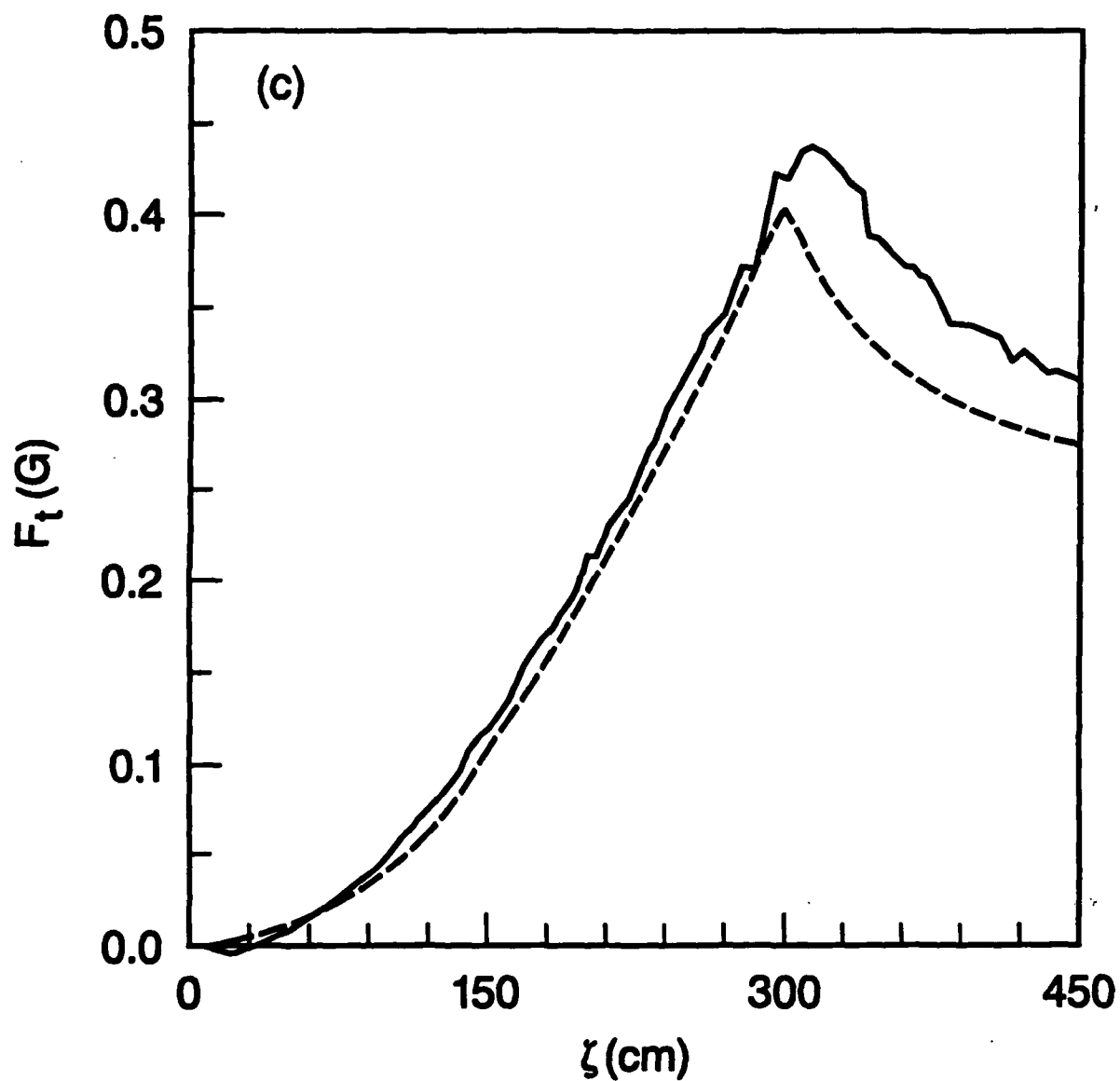= 2$, $q = 0.2$, $\delta = 0.1$, and $p = 1$. The lengths y_c and r_c are normalized to the beam radius, $r_b = 1$ cm.

44

Fig. 4b — Typical comparison plots of the total numerical tracking force F_t [solid line] and the theoretical magnetic force F_{tm} [dashed line] for $y_c = 3$, $r_c = 1$, $q = 0.1$, $\delta = 0.1$, and $p = 1$.
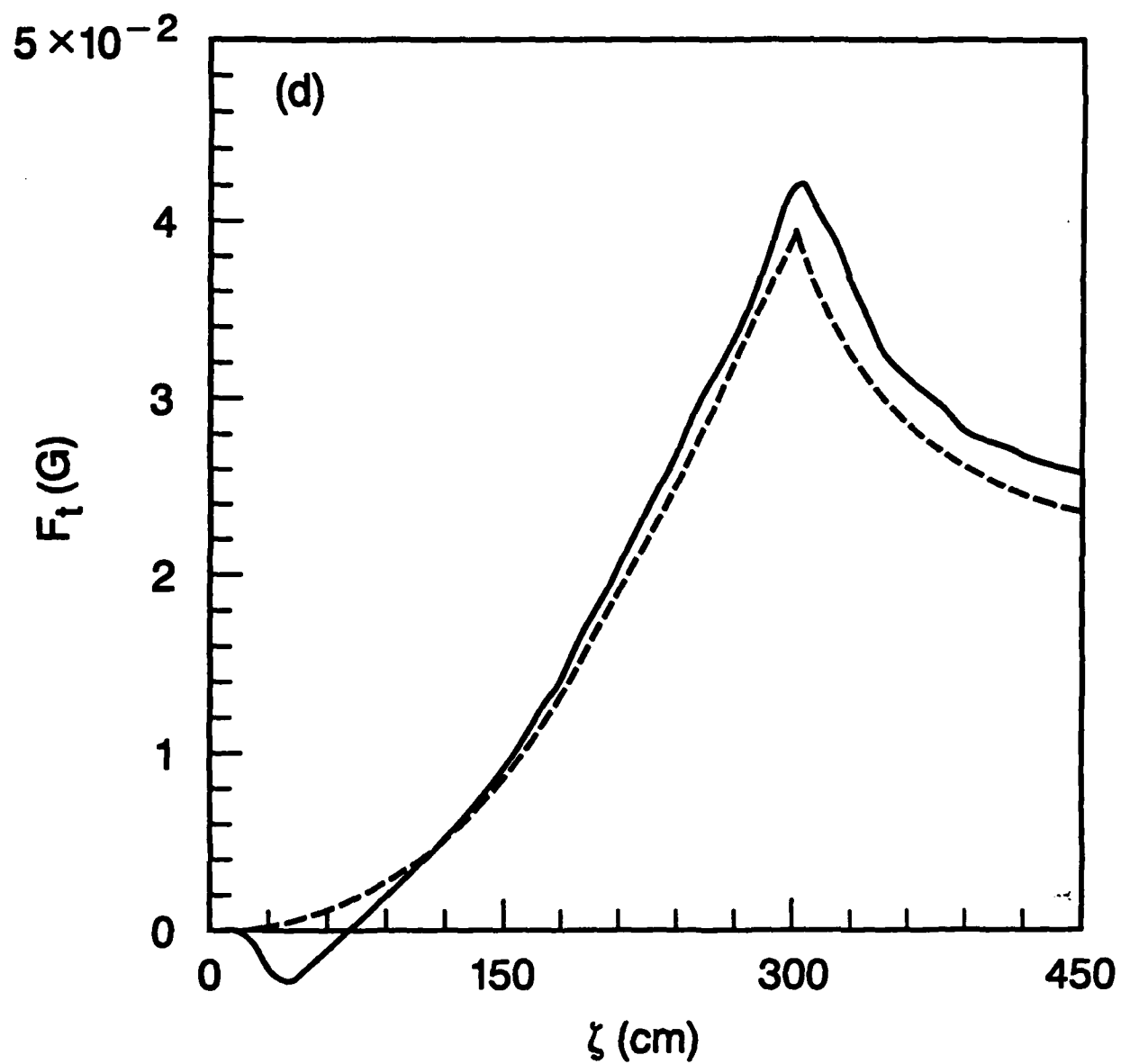
Fig. 4c — Typical comparison plots of the total numerical tracking force, F_t [solid line] and the theoretical magnetic force F_{tm} [dashed line] for $y_c = 0.1$, $r_c = 0.5$, $q + 0.4$, $\delta = 10^{-5}$, and $p = 0.2$.

46

Fig. 4d — Typical comparison plots of the total numerical tracking force F_t [solid line] and the theoretical magnetic force F_{tm} [dashed line] for $y_c = 0.1$, $r_c = 2$, $q = 0.01$, $\delta = 0.63$, and $p = 5$.
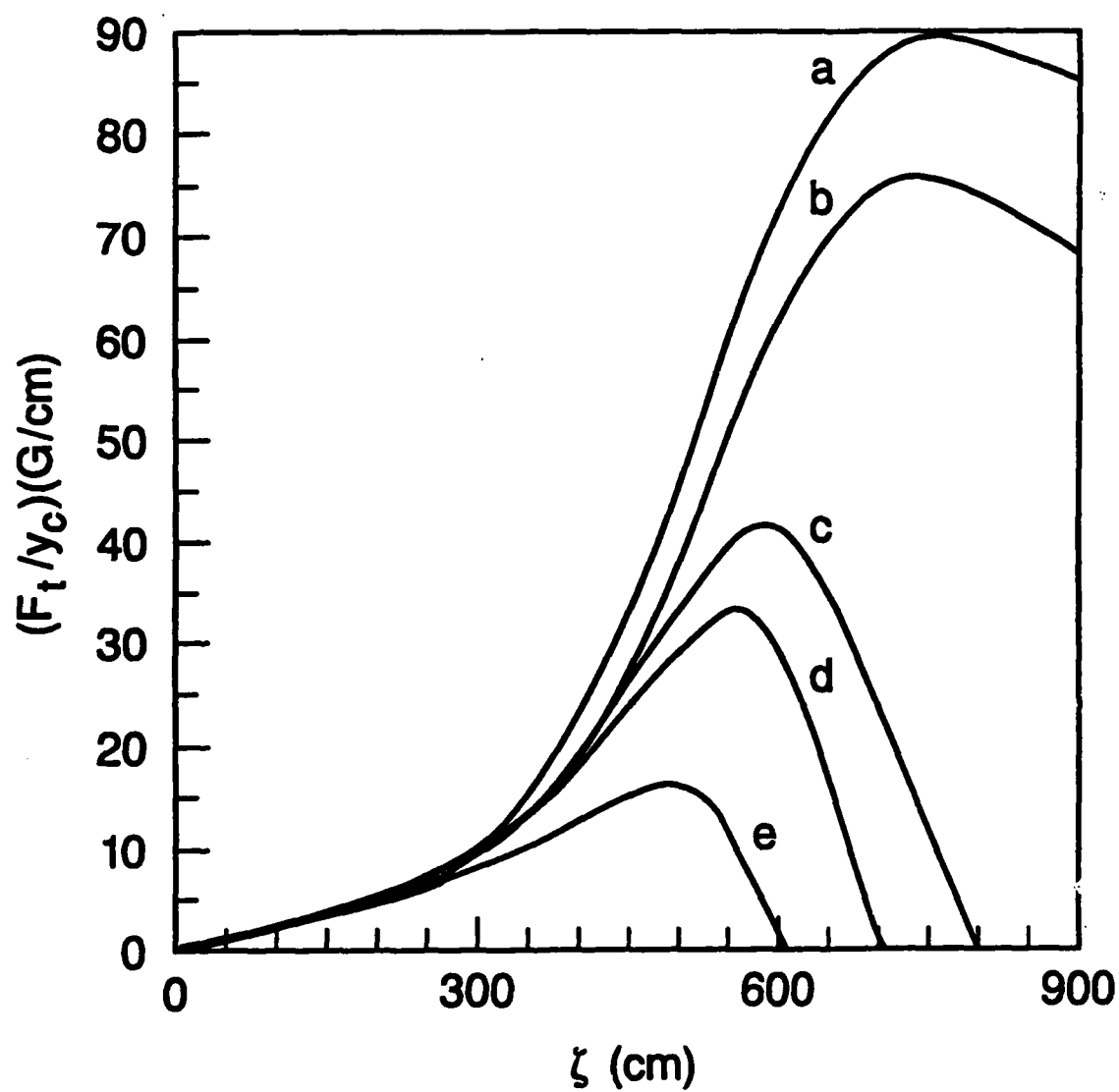
47

Fig. 5 — The density force F_ζ as a function of air chemistry: (a) beam impact ionization only; (b) attachment; (c) electron-ion recombination; (d) Spitzer collisions; and (e) all of the above.